PHYSICAL REVIEW B **90**, 161108(R) (2014)

Engineering relativistic effects in ferroelectric SnTe

E. Plekhanov,[1] P. Barone,[1] D. Di Sante,[1,2] and S. Picozzi[1]
[1]*Consiglio Nazionale delle Ricerche - CNR-SPIN, I-67100 L'Aquila, Italy*
[2]*Department of Physical and Chemical Sciences, University of L'Aquila, Via Vetoio, I-67100 L'Aquila, Italy*
(Received 3 February 2014; revised manuscript received 8 May 2014; published 28 October 2014)

Spin-orbit coupling is increasingly seen as a rich source of novel phenomena, as shown by the recent excitement around topological insulators and Rashba effects. We here show that the addition of ferroelectric degrees of freedom to a semiconductor featuring topologically nontrivial properties, such as SnTe, merges the intriguing field of spin-orbit-driven physics with nonvolatile functionalities appealing for spintronics. By using a variety of modeling techniques, we show that a strikingly rich sequence of phases can be induced in SnTe, when going from a room-temperature cubic phase to a low-temperature ferroelectric structure, ranging from a topological crystalline insulator to a time-reversal-invariant Z_2 topological insulator to a "ferroelectric Rashba semiconductor," exhibiting a huge electrically controllable Rashba effect in the bulk band structure.

DOI: 10.1103/PhysRevB.90.161108 PACS number(s): 71.20.−b, 71.70.Ej, 73.20.−r

Many of the materials science topics that have recently drawn much attention arise from the intriguing physics based on spin-orbit coupling (SOC). For example, growing enthusiasm is devoted to the so-called "Ferroelectric Rashba Semiconductors" (FERSCs), a novel class of multifunctional materials featuring GeTe as a prototype [1,2]. In FERSCs, a (giant) Rashba effect (RE) is present in the *bulk* band structure and is intimately linked to ferroelectricity: the spin-texture can be fully reversed when switching the ferroelectric (FE) polarization. Indeed, in Ref. [1] some of the present authors predicted, by means of first-principles simulations, that FE GeTe would show a huge Rashba spin splitting for the valence band maximum and an unprecedented Rashba parameter. While our theoretical predictions for GeTe urgently call for an experimental confirmation, the fascinating FERSC phenomenology opens exciting perspectives in electrically controlled semiconductor spintronics; for example, a modified Datta-Das spin transistor based on a FERSC channel would allow the appealing integration of storage and logic functionalities [1].

Moreover, over the last few years topological insulators (TIs) [3] have been at the center of increasing excitement, due to exotic properties, such as their surface states (SSs) showing a Dirac spectrum and being exceptionally robust against perturbations. TIs possess a nontrivial Z_2 classification, arising from an odd number of SOC-induced band inversions in their bulk band structure. The SOC-related origin of the phenomenon makes the SSs show a single spin state for each momentum, paving the way to spin-polarized currents of interest in spintronics. Recently, a novel class of TI has been introduced, namely topological crystalline insulators (TCIs) [4], where metallic edge states are protected by point- or space-group symmetries, rather than time-reversal (TR) symmetry as in usual Z_2 TIs. The proof of the existence of TCIs came from rocksalt SnTe [5,6] (and related alloys [7,8]), where the *fcc* lattice shows a (110) mirror plane and the (bulk) L symmetry point features a SOC-induced band inversion between anion and cation in the valence-band maximum (VBM) and conduction-band minimum (CBM), compared to other standard semiconductors. Surfaces preserving the mirror operation, such as the (001), were first predicted (and later experimentally confirmed via angle-resolved photoemission) to show an even number of Dirac branches along the $\overline{\Gamma}$-$\overline{X}$ direction, corresponding to an even number of band inversions (rather than an odd number, as in standard TIs).

In this work, we focus on the coexistence and interplay between FERSC characteristics and topological behavior, starting from the observation that any material showing at the same time ferroelectricity and a topologically nontrivial character is likely to show large SOC and a small band gap: it is therefore expected to satisfy also the conditions for a (possibly large) bulk RE. A multifunctional material being at the same time a FERSC *and* a TCI would clearly constitute a breakthrough in the field and we show here that this is the case of SnTe. The role of displacements in TCI was only marginally discussed in Ref. [5] for SnTe, where a FE distortion along the [111] direction was considered (consistently with crystalline rhombohedral deformation, occurring at low temperatures [9]). While Hsieh *et al.* [5] performed helpful symmetry considerations, they remained at the speculative level. Rather, we here show that it is important to perform a quantitative analysis. In closer detail, by means of *ab initio* simulations, we consider the transition from cubic to FE SnTe and explore topological properties along the path connecting the two extremal phases, by focusing on [111] surfaces. Indeed, several exciting outcomes result: (i) below the FE transition temperature, SnTe turns out to be a novel FERSC; (ii) the TCI phase for the cubic rocksalt structure can be turned to a Z_2 TI under external manipulation; and (iii) the coexistence of FERSC behavior with either TCI or Z_2 topological insulating phases is shown to occur.

Technical details. Density functional theory (DFT) simulations were performed using the Vienna Ab initio Simulation Package (VASP) [10] and the Generalized Gradient Approximation (GGA) [11] in the Perdew-Burke-Ernzerhof (PBE) formalism for the exchange-correlation potential. We used an energy cutoff for the plane wave basis of 400 eV and a $16 \times 16 \times 16$ Monkhorst-Pack k-point mesh [12]. Test calculations using more accurate hybrid functionals within the HSE [13] formalism (see [14]) showed that the relevant physics was only marginally affected, so we will focus here on the GGA results. We here concentrate on the [111]

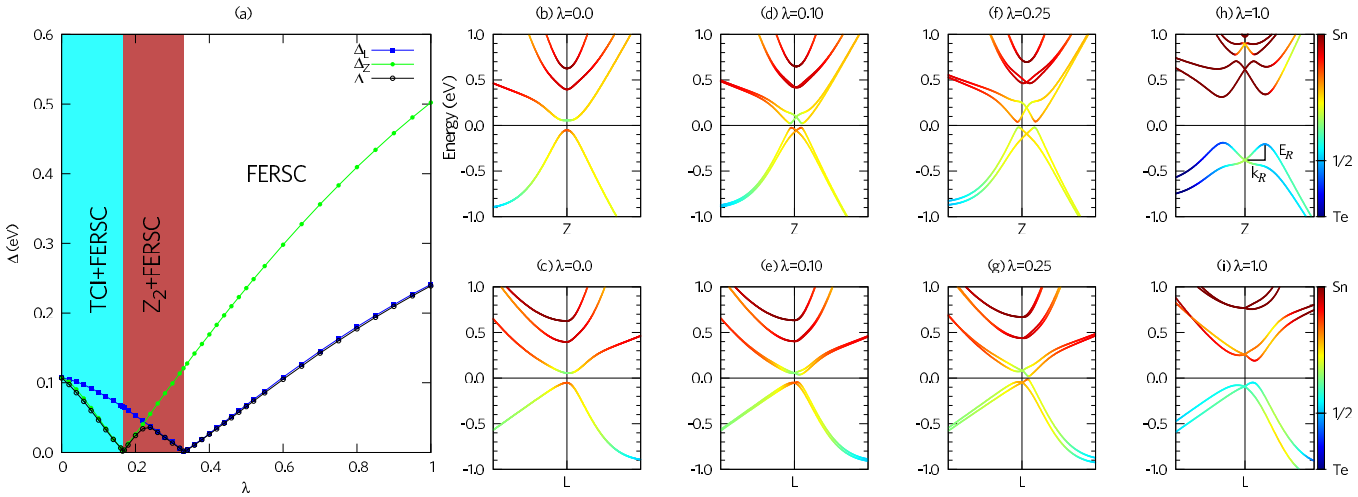

FIG. 1. (Color online) *Ab initio* DFT. (a) Topological phase diagram estimated from the evolution, as a function of λ, of the energy gaps around Z (Δ_Z) and to L (Δ_L). The "minimal" energy gap (Δ) over the whole BZ is drawn in black. The band structures in proximity to Z (along the directions $B \to Z \to P$) and L (along the directions $\Gamma \to L \to B_1$), respectively, are shown in panels (b) and (c) for $\lambda = 0.0$, in panels (d) and (e) for $\lambda = 0.10$, in panels (f) and (g) for $\lambda = 0.25$, in panels (h) and (i) for $\lambda = 1.0$. The orbital character of bands is shown by color map going from dark blue (Te) to dark red (Sn), with 1/2 corresponding to the equally mixed anionic and cationic character. For clarity, we report in panel (h) the graphical definition of the Rashba momentum offset, k_R, and of the Rashba energy splitting, E_R.

surface, usually a natural cleavage plane for rhombohedral crystals. To calculate the (111) SS in the slab geometry, the number of layers has to be sufficiently large to distinguish the surface from the bulk states which makes *ab initio* approaches prohibitive. We therefore resorted to an effective tight-binding (TB) model for SSs. The TB hopping matrix elements were determined by projection of the *ab initio* VASP Hamiltonian onto the Maximally Localized Wannier Orbitals (MLWOs) through the WANNIER90 package [15]. As for structural parameters, we employed those optimized within DFT-GGA. For the rhombohedral (cubic) structure, we used lattice constants $a = 6.475$ Å (6.420 Å), rhombohedral angles $\alpha = 58.8^\circ$ (60°), and atomic displacements (in internal units) $\tau = 0.026(0)$ (see Sec. A and Table 1 of the Supplemental Material [14]).

Bulk electronic structure. As already mentioned, the cubic phase of SnTe is a TCI, while the rhombohedral phase is FE (with a calculated polarization of $\sim 40\ \mu C/cm^2$; see Supplemental Material [14]). We here search for an intermediate phase (allowed by symmetry) which exhibits both ferroelectricity and RE, being at the same time topologically nontrivial. In order to demonstrate the existence of such a phase, we construct a path, parametrized by λ, linearly connecting the structural parameters (i.e., in terms of lattice constants and angles, atomic positions, etc.) of the cubic TCI phase (space group $Fm3m$, $\lambda = 0$) to the rhombohedral FE one (space group $R3m$, $\lambda = 1$). Our DFT calculations are reported in Fig. 1, where we show the energy gaps at the Z and L points of the rhombohedral Brillouin zone (BZ), along with a zoom of the related band structures, for different values of λ.

Let us first discuss the FERSC behavior. As for GeTe [1], SnTe meets all the necessary conditions pointed out to support a giant RE. Specifically, the VBM and CBM, both at Z and L points, have the same symmetry character coming from an unusual band ordering close to the Fermi level. This, in combination with a rather strong SOC, a very small gap, and the lack of inversion symmetry, paves the way for a huge electrically controllable bulk Rashba spin splitting [16] (RSS); in the low-temperature phase ($\lambda = 1$), we calculated a Rashba momentum offset, around Z, $k_R \approx 0.08$ Å^{-1}. The energy splitting at Z, E_R [calculated as the energy difference between the lowest conduction (highest valence) band at k_R and at the high symmetry points (HSPs) Z] is as large as 272 (172) meV for the conduction (valence) bands; see Fig. 1(h). The Rashba parameter α_R being as large as 6.8 (4.4) eV/Å for the conduction (valence) bands, SnTe is unambiguously proven to be an additional example of FERSC for all values $\lambda > 0$ (see Sec. B and Fig. 1 of the Supplemental Material [14] for further details). Moreover, differently from GeTe [1], in SnTe the VBM and CBM at Z both belong to the $j = 1/2$ manifold (at variance with $j = 1/2$ and $j = 3/2$ for VBM and CBM, respectively, in GeTe). Therefore, SnTe seems even more promising than GeTe, as the large RSS occurs both in the valence and in the conduction bands, opening the routes towards an ambipolar behavior [17] of interest for spintronics.

As for the topological properties, let us remark that, along the whole λ path, SnTe is characterized by the presence of a band gap among different Rashba peaks, k_R, around either L or Z. The key point is, however, the band structure evolution, as a function of λ, of the Z and L points, the two being different because of the rhombohedral/off-centering distortions. By looking at the inverted orbital character (typical for TIs), we note that the TCI phase survives the rhombohedral distortion for quite long [up to $\lambda = 0.16$; cf. Fig. 1(a)]. In this range, ferroelectricity coexists with a small RSS, mainly located at Z; we therefore label this phase as TCI+FERSC. For the critical value, $\lambda = 0.16$, the gap closes at Z. Upon larger displacements, the gap at Z reopens without band inversion, whereas at L the band inversion is still present. In this range of λ, an extremely exotic phase exists: along with the FERSC behavior, an odd number of band inversions

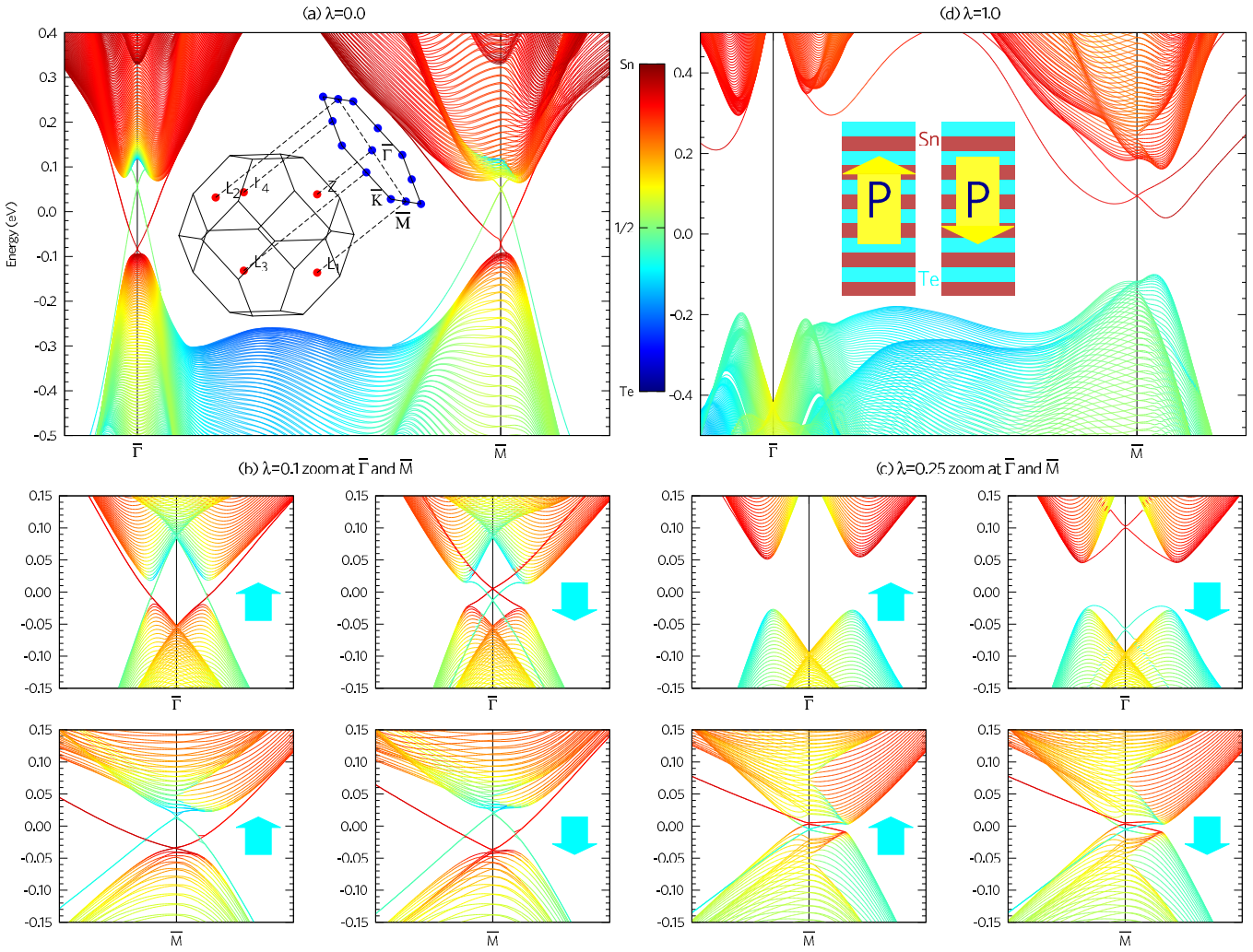

FIG. 2. (Color online) TB + MLWO. (a) [111] SBS for $\lambda = 0.0$. The inset shows the rhombohedral BZ and its projection on the [111] surface. (d) [111] SBS for $\lambda = 1.0$. The inset shows the stacking sequence of the unit cells, along with the two possible terminations and directions of polarization (labeled as $P_\uparrow$ in the left and $P_\downarrow$ in the right). (b) and (c) show the SBS for $\lambda = 0.1$ and $\lambda = 0.25$. In the latter panels, there are four subpanels, showing the band structure around $\overline{\Gamma}$ for $P_\uparrow$ (upper left), around $\overline{\Gamma}$ for $P_\downarrow$ (upper right), around $\overline{M}$ for $P_\uparrow$ (lower left), around $\overline{M}$ for $P_\downarrow$ (lower right). All the calculations were performed on slabs with 480 Sn and Te layers, except for the case of $\lambda = 0.25$ and around $\overline{M}$ point (where higher accuracy is needed), in which 720-layer slabs were used. Color scale as in Fig. 1.

opens the possibility for a Z_2-type of TI. This phase, labeled as Z_2+FERSC, is indeed confirmed to be a strong TI from the evaluation of the Z_2 topological indices as (1,111) (see Sec. C of the Supplemental Material [14] for details). Finally, a further increase in λ closes the gap (at $\lambda = 0.33$) at the Rashba points k_R in the vicinity of L, thus switching the band inversion off (along with the TI regime) at L. The system consequently becomes a trivial FE insulator with strong RE (i.e., a *topologically trivial* FERSC). The sequence of phases (TCI+FERSC, Z_2+FERSC, FERSC), shown in Fig. 1(a), is the main result of this Rapid Communication, further explored below in terms of surface electronic structure.

Surface states. Owing to the bulk-boundary correspondence (BBC), all the findings about topological states in the bulk find their counterparts in the electronic properties of the [111] SS, showing intriguing aspects related to ferroelectricity. Since the FE polarization is perpendicular to the (111) surface [18], in the slab geometry with mixed termination (Te on one side, Sn on the other) two possibilities can be distinguished: one, when polarization points from the inner layers towards the Sn surface (and away from the Te surface) or the other, when it points away from the Sn surface (and towards the Te surface), as shown in the inset of Fig. 2(d). Due to the mixed termination, the contributions of each surface can be distinguished by looking at their orbital and atomic character. We underline that the presence or absence of the topological SS is indeed a "bulk"-derived property, marginally depending on the surface band structure (SBS) or on the presence of surface defects. As a matter of fact, the topological nature of a band insulator is routinely assessed by calculating SSs in a slab geometry, often in the framework of empirical TB models [8,19]. Here, we use a much more realistic TB parametrization derived from an accurate first-principles-based Wannier procedure.

As is well known, in the SnTe cubic phase, each surface of the slab exhibits a cone of SSs at $\overline{\Gamma}$ and each of the three nonequivalent $\overline{M}$ points of the surface Brillouin zone [cf. inset in Fig. 2(a)], consistent with the existing literature [20,21] and

with the band inversion observed in the bulk bands. It is worth noting that Sn surface cones cross in the vicinity of the VBM, while the Te SSs cross close to the CBM.

In the TCI+FERSC phase ($0 < \lambda < 0.16$), the system shows a finite FE polarization but is topologically equivalent to the cubic one; i.e., we find in the surface electronic structure the same number of cones at the same symmetry points for $\lambda = 0.0$ and 0.1 [cf. Fig. 2(a) and 2(b)]. However, for a finite λ, the behavior at $\overline{\Gamma}$ depends on the polarization direction: the crossing can either occur close to the middle of the gap [cf. Fig. 2(b), upper right panel] or closer to crossing of projected bulk bands [cf. Fig. 2(b), upper left panel]. This allows for an additional control of the surface electronic properties through an electric field.

In the Z_2+FERSC phase ($0.16 < \lambda < 0.33$), the inverted (normal) gap at L (Z) is reflected on the surface electronic structure [cf. Fig. 2(c)]. The striking feature of this phase is the presence of a single Dirac cone from each surface crossing at $\overline{M}$. Since the number of nonequivalent Dirac cones is odd, this phase is confirmed to be a Z_2 TR-invariant strong TI with indices (1,111). The bulk bands (projected at the surface) exhibit a strong RE at $\overline{\Gamma}$ and a tiny one at $\overline{M}$. Although the SBS at $\overline{M}$ does not depend on the FE polarization direction, at $\overline{\Gamma}$ it does. Indeed, for polarization corresponding to the negative shift of the Te sublattice with respect to the Sn one, a *surface RE* appears. We recall, in fact, that the RE discussed so far in this Rapid Communication occurs in the *bulk*; however, a more "conventional" RE can also occur at the *surface*, deriving from the breaking of inversion symmetry induced by the presence of any surface.

Recall now that, in the bulk, the phase at $\lambda > 0.33$ does not show any band inversion and is topologically trivial. This phase also characterizes the final end point of our adiabatic path at $\lambda = 1$ (FERSC phase), for which we show the SBS in Fig. 2(d). Here, the bulk RE is evident both at $\overline{\Gamma}$ and $\overline{M}$, while the surface RE is present on one of the two HSPs depending on the orientation of polarization.

In summary, we have addressed the intriguing physics brought by SOC interlinked with ferroelectricity in SnTe. By means of a combination of DFT, TB, and Wannier orbitals, we analyzed bulk and surface electronic structures and showed that, upon any external agent (such as pressure, strain, or chemical doping) that is able to drive a transition from the room-temperature cubic centrosymmetric structure to the low-temperature FE structure of SnTe, an exotic sequence of peculiar phases can be induced, controlled, and optimized. Indeed, these phases range from a TCI for small deformations ($0 < \lambda < 0.16$) to a Z_2 topological insulator for slightly larger FE distortions ($0.16 < \lambda < 0.33$) to a trivial topological behavior up to the experimental FE structure ($0.33 < \lambda < 1$). Moreover, we show that topological phases can coexist with a FERSC behavior, where a strong RSS is predicted to occur in the bulk electronic structure and whose spin texture is controllable via an electric field. While the specific range of λ values for each phase depends on model details, we predict the *sequence of phases*—as a function of λ—from TCI over Z_2 to trivial insulator with strong RE, to be quite general. Regarding the possibility to experimentally observe the intermediate phases, we note that the parameter λ, connecting the cubic and the rhombohedral phases, is mainly related to the ferroelectric displacement between Sn and Te sublattices and, hence, can be controlled by several means, such as p doping or chemical substitution. Indeed, the naturally occurring p-type doping in SnTe, due to Sn vacancies, strongly affects FE properties. For example, p doping above a critical threshold [9] completely destroys the displacement. In addition, it has been theoretically argued that n-type doping could smoothly tune the atomic displacement in the prototypical FE, $BaTiO_3$ [22]. Analogously, the study of isovalent substitution in SnGeTe [23] showed that the displacement can be controlled by tuning the concentration of Sn.

While our results urgently call for an experimental verification, it is clear that the multifunctional behavior of FE SnTe shows a wide tunability through a variety of different topological insulating or FERSC phases. More generally, our work shows how the peculiar interplay among ferroelectricity, SOC, topology, and RE opens exciting perspectives in different key areas in current science, ranging from fundamental condensed matter physics (in terms of microscopic mechanisms) to materials science (in terms of novel and advanced compounds) to technology (in terms of a new generation of electrically controlled spintronic devices).

We acknowledge computational support through the PRACE project "TRASFER", awarding us access to resource MareNostrum based in Spain at Barcelona Supercomputing Center (BSC-CNS), CINECA facilities available through the ISCRA initiative (FeBTOMEC project), and the Supercomputing Cluster at CNR-SPIN SA (CLUSA).

[1] D. Di Sante, P. Barone, R. Bertacco, and S. Picozzi, Adv. Mater. **25**, 509 (2013); **25**, 3625 (2013).

[2] S. Picozzi, Front. Phys. **2**, 10 (2014).

[3] See for example M. Z. Hasan and C. L. Kane, Rev. Mod. Phys. **82**, 3045 (2010); X. L. Qi and S. C. Zhang, *ibid.* **83**, 1057 (2011); J. E. Moore, Nature (London) **464**, 194 (2010); L. Fu, C. L. Kane, and E. J. Mele, Phys. Rev. Lett. **98**, 106803 (2007).

[4] L. Fu, Phys. Rev. Lett. **106**, 106802 (2011).

[5] T. H. Hsieh, H. Lin, J. Liu, W. Duan, A. Bansil, and L. Fu, Nat. Commun. **3**, 982 (2012).

[6] Y. Tanaka, Zhi Ren, T. Sato, K. Nakayama, S. Souma, T. Takahashi, K. Segawa, and Y. Ando, Nat. Phys. **8**, 800 (2012).

[7] S. Y. Xu, C. Liu, N. Alidoust, M. Neupane, D. Qian, I. Belopolski, J. D. Denlinger, Y. J. Wang, H. Lin, L. A. Wray, G. Landolt, B. Slomski, J. H. Dil, A. Marcinkova, E. Morosan, Q. Gibson, R. Sankar, F. C. Chou, R. J. Cava, A. Bansil, and M. Z. Hasan, Nat. Commun. **3**, 1192 (2012).

[8] P. Dziawa, B. J. Kowalski, K. Dybko, R. Buczko, A. Szczerbakow, M. Szot, E. Łusakowska, T. Balasubramanian, B. M. Wojek, M. H. Berntsen, O. Tjernberg, and T. Story, Nat. Mater. **11**, 1023 (2012).

[9] M. Iizumi, Y. Hamaguchi, K. F. Komatsubara, and Y. Kato, J. Phys. Soc. Jpn. **38**, 443 (1975).

[10] G. Kresse and D. Joubert, Phys. Rev. B **59**, 1758 (1999).

[11] J. P. Perdew, K. Burke, and M. Ernzerhof, Phys. Rev. Lett. **77**, 3865 (1996).

[12] J. Monkhorst and J. D. Pack, Phys. Rev. B **13**, 5188 (1976).

[13] J. Heyd, G. E. Scuseria, and M. Ernzerhof, J. Chem. Phys. **118**, 8207 (2003); **124**, 219906(E) (2006).

[14] See Supplemental Material at http://link.aps.org/supplemental/10.1103/PhysRevB.90.161108 for additional details on structural, electronic, and ferroelectric properties, on the Rashba effect, and on the evaluation of Z_2 topological invariants.

[15] A. Mostofi, J. R. Yates, Y.-S. Lee, I. Souza, D. Vanderbilt, and N. Marzari, Comput. Phys. Commun. **178**, 685 (2008).

[16] M. S. Bahramy, R. Arita, and N. Nagaosa, Phys. Rev. B **84**, 041202(R) (2011).

[17] A. Crepaldi, L. Moreschini, G. Autès, C. Tournier-Colletta, S. Moser, N. Virk, H. Berger, Ph. Bugnon, Y. J. Chang, K. Kern, A. Bostwick, E. Rotenberg, O. V. Yazyev, and M. Grioni, Phys. Rev. Lett. **109**, 096803 (2012).

[18] In the case of FE GeTe, structurally very close to SnTe, the polarization has been suggested, both theoretically using first-principle calculations and experimentally via PFM measurements, to be intrinsically perpendicular to the GeTe(111) thin films' surfaces. See V. L. Deringer, M. Lumeij, and R. Dronskowski, J. Phys. Chem. **116**, 15801 (2012) ; C. Rinaldi *et al.* (unpublished).

[19] B. M. Wojek, R. Buczko, S. Safaei, P. Dziawa, B. J. Kowalski, M. H. Berntsen, T. Balasubramanian, M. Leandersson, A. Szczerbakow, P. Kacman, T. Story, and O. Tjernberg, Phys. Rev. B **87**, 115106 (2013); C. M. Polley, P. Dziawa, A. Reszka, A. Szczerbakow, R. Minikayev, J. Z. Domagala, S. Safaei, P. Kacman, R. Buczko, J. Adell, M. H. Berntsen, B. M. Wojek, O. Tjernberg, B. J. Kowalski, T. Story, and T. Balasubramanian, *ibid.* **89**, 075317 (2014).

[20] J. Liu, W. Duan, and L. Fu, Phys. Rev. B **88**, 241303 (2013).

[21] S. Safaei, P. Kacman, and R. Buczko, Phys. Rev. B **88**, 045305 (2013).

[22] Y. Wang, X. Liu, J. D. Burton, S. S. Jaswal, and E. Y. Tsymbal, Phys. Rev. Lett. **109**, 247601 (2012).

[23] A. I. Lebedev, I. A. Sluchinskaya, V. N. Demin, and I. H. Munro, JETP Lett. **63**, 635 (1996); Phase Transitions **60**, 67 (1997).